Defense Technical Information Center Compilation Part Notice

ADP023840

TITLE: Time-Accurate Aerodynamic Modeling of Synthetic Jets for Projectile Control

DISTRIBUTION: Approved for public release, distribution unlimited

This paper is part of the following report:

TITLE: Proceedings of the HPCMP Users Group Conference 2004. DoD High Performance Computing Modernization Program [HPCMP] held in Williamsburg, Virginia on 7-11 June 2004

To order the complete compilation report, use: ADA492363

The component part is provided here to allow users access to individually authored sections of proceedings, annals, symposia, etc. However, the component should be considered within the context of the overall compilation report and not as a stand-alone technical report.

The following component part numbers comprise the compilation report:
ADP023820 thru ADP023869

Time-Accurate Aerodynamic Modeling of Synthetic Jets for Projectile Control

Jubaraj Sahu

US Army Research Laboratory (ARL), Aberdeen Proving Ground, MD
sahu@arl.army.mil

Abstract

This paper describes a computational study undertaken to determine the aerodynamic effect of tiny unsteady synthetic jets as a means to provide the control authority needed to maneuver a spinning projectile at low subsonic speeds. Advanced Navier-Stokes computational techniques have been developed and used to obtain numerical solutions for the unsteady jet-interaction flow field at subsonic speeds and small angles of attack. Unsteady numerical results show the effect of the jet on the flow field and on the aerodynamic coefficients. The unsteady jet is shown to substantially alter the flow field both near the jet and the base region of the projectile that in turn affects the forces and moments even at zero degree angle of attack. The results have shown the potential of computational fluid dynamics to provide insight into the jet interaction flow fields and provided guidance as to the locations and sizes of the jets to generate the maximum control authority to maneuver a projectile to hit its target with precision.

1. Introduction

Accurate determination of aerodynamics is critical to the low-cost development of new advanced munitions[1,2]. Competent smart munitions that can more accurately hit a target can greatly increase lethality and enhance survivability. Desert storm convincingly demonstrated the value of large-scale precision-guided munitions. A similar capability for small-scale munitions would increase the effectiveness of the infantry units, reduce collateral damage, and reduce the weight of munitions that must be carried by individual soldiers. The Army is therefore, seeking a new generation of autonomous, course-correcting, gun-launched projectiles for infantry soldiers. Due to small projectile diameter (20 to 40mm), maneuvers by canards and fins seem very unlikely. *An alternate and new evolving technology* is the micro-adaptive flow control through synthetic jets. These very tiny (of the order of 0.3mm) synthetic micro-jet actuators

have been shown to successfully modify subsonic flow characteristics and pressure distributions for simple airfoils and cylinders[3,4]. The synthetic jets (fluid being pumped in and out of the jet cavity at a high frequency of the order of 1000 Hz) are control devices (Figure 1) with zero net mass flux and are intended to produce the desired control of the flow field through momentum effects. Many parameters such as jet location, jet velocity, and jet actuator frequency can affect the flow control phenomenon. Up to now, the physics of this phenomenon has not been well understood and advanced numerical predictive capabilities or high fidelity computational fluid dynamics (CFD) design tools did not exist for simulation of these unsteady jets. However, the research effort described here has advanced the aerodynamic numerical capability to accurately predict and provide a crucial understanding of the complex flow physics associated with the unsteady aerodynamics of this new class of tiny synthetic micro-jets for control of modern projectile configurations. High performance CFD techniques were developed and applied for the design and analysis of these Micro-Adaptive Flow Control systems for steering a spinning projectile for infantry operations.

The control of the trajectory of a 40mm spinning projectile is achieved by altering the pressure distribution on the projectile through *forced* asymmetric flow separation. Unsteady or time-accurate CFD modeling capabilities were developed and used to assist in the design of the projectile shape, the placement of the synthetic actuators and the prediction of the aerodynamic force and moments for these actuator configurations. Additionally, the advanced CFD capabilities provided a simpler way to explore various firing sequences of the actuator elements. Time-accurate unsteady CFD computations were performed to predict and characterize the unsteady nature of the synthetic jet interaction flow field produced on the M203 grenade launched projectile for various yaw and spin rates for fully viscous turbulent flow conditions. Turbulence was initially modeled using a traditional Reynolds-Averaged Navier-Stokes (RANS) approach. Although, this approach provided some detailed flow physics, it was found to be less accurate for

144

this new class of unsteady flows associated with synthetic jets. In order to improve the accuracy of the numerical simulation, the predictive capability was extended to include a higher order hybrid RANS/LES (Large Eddy Simulation) approach[5,6]. This new approach computes the large eddies present in the turbulent flow structure and allowed the simulation to capture, with high fidelity, additional flow structures associated with the synthetic jet interactions in a time-dependent fashion. Modeling of azimuthally placed synthetic micro-jets required tremendous grid resolution, highly specialized boundary conditions for the jet activation, and the use of advanced hybrid LES approachs permitting local resolution of the unsteady turbulent flow with high fidelity. The addition of yaw and spin while the projectile is subjected to the pulsating micro-jets rendered predicting forces and moments a major challenge. The Department of Defense High Performance Computing Modernization Office selected this research as a *DoD Challenge Project* and provided the massive computational resources required by these unsteady time-accurate simulations. The new capability has been demonstrated and this technology has recently been successfully applied to the self-correcting projectile for infantry operations (SCORPION) program.

2. Computational Methodology

The complete set of three-dimensional (3-D) time-dependent Navier-Stokes equations[7] is solved in a time-accurate manner for simulations of unsteady synthetic jet interaction flow field on the M203 grenade launched projectile with spin. The 3-D time-dependent Reynolds-averaged Navier-Stokes (RANS) equations are solved using the finite volume method[8]:

$$\frac{\partial}{\partial t} \int_V \mathbf{W} dV + \oint [\mathbf{F} - \mathbf{G}] \cdot dA = \int_V \mathbf{H} dV \qquad (1)$$

where $\mathbf{W}$ is the vector of conservative variables, $\mathbf{F}$ and $\mathbf{G}$ are the inviscid and viscous flux vectors, respectively, $\mathbf{H}$ is the vector of source terms, V is the cell volume, and A is the surface area of the cell face.

Second-order discretization was used for the flow variables and the turbulent viscosity equations. Two-equation[9] and higher order hybrid RANS/LES[6] turbulence models were used for the computation of turbulent flows. The hybrid RANS/LES approach based on Limited Numerical Scales (LNS) is well suited to the simulation of unsteady flows and contains no additional empirical constants beyond those appearing in the original RANS and LES sub-grid models. With this method a regular RANS-type grid is used except in isolated flow regions where denser, LES-type mesh is used to resolve critical unsteady flow features. The hybrid model

transitions smoothly between an LES calculation and a cubic k-ε model, depending on grid fineness. A somewhat finer grid was placed around the body, and near the jet, the rest of the flow field being occupied by a coarser, RANS-like mesh. Dual time-stepping was used to achieve the desired time-accuracy. In addition, special jet boundary conditions were developed and used for numerical modeling of synthetic jets. Grid was actually moved to take into account the spinning motion of the projectile.

3. Projectile Geometry and Computational Grid

The projectile used in this study is a 1.8-caliber ogive-cylinder configuration (see Figure 2). Here, the primary interest is in the development and application of CFD techniques for accurate simulation of a projectile flow field in the presence of unsteady jets. The first step here was to obtain a converged solution for the projectile without the jet. A converged jet-off solution was then used as the starting condition for the computation of time-accurate unsteady flow field for the projectile with synthetic jets. The jet locations on the projectile are shown in Figure 3. The jet conditions were specified at the exit of the jet for the unsteady (sinusoidal variation in jet velocity) jets. The jet conditions specified include the jet pressure, density, and velocity components. Numerical computations have been made for these jet cases at subsonic Mach numbers, M = 0.11 and 0.24 and at angles of attack, α = 0° to 4°. The jet width was 0.32 mm, the jet slot half-angle was 18°, and the peak jet velocities used were 31 and 69 m/s operating at a frequency of 1000 Hz.

A computational grid expanded near the vicinity of the projectile is shown in Figure 4. Grid points are clustered near the jet as well as the boundary layer regions to capture the high gradients flow regions. The computational grid has 211 points in the streamwise direction, 241 in the circumferential direction, and 80 in the normal direction. The unsteady simulation took thousands of hours of CPU time on Silicon Graphics Origin and IBM SP3 computers running with 16–24 processors.

4. Results

Time-accurate unsteady numerical computations using advanced viscous Navier-Stokes methods were performed to predict the flow field and aerodynamic coefficients on both a non-spinning and a spinning projectile. Limited experimental data[11,12] exists only for the non-spinning case and was used to validate the unsteady CFD results.

4.1. Non-spinning Projectile Case.

3-D unsteady CFD results were obtained at a subsonic Mach number of 0.11 and several angles of attack from 0° to 4° using both RANS and the hybrid RANS/LES approaches. These 3-D unsteady CFD results have provided fundamental understanding of fluid dynamics mechanisms associated with the interaction of the unsteady synthetic jets and the projectile flow fields. Many flow field solutions resulting from the simulation of multiple spin cycles and, hence, a large number of synthetic jet operations, were saved at regular intermittent time-intervals to produce movies to gain insight into the physical phenomenon resulting from the synthetic jet interactions. The unsteady jets were discovered to break up the shear layer coming over the step in front of the base of the projectile. It is this insight that was found to substantially alter the flow field (making it unsteady) both near the jet and in the wake region that in turn produced the required forces and moments even at zero degree angle-of-attack (level flight). Time-accurate velocity magnitude contours (Figures 5 and 6) confirm the unsteady wake flow fields arising from the interaction of the synthetic jet with the incoming free stream flow at Mach = .11. Figure 7 shows the particles emanating from the jet and interacting with the wake flow making it highly unsteady. More importantly, the break up of the shear layer is clearly evidenced by the particles clustered in regions of flow gradients or vorticity (evident in computed pressure contours, Figure 8). Verification of this conclusion is provided by the excellent agreement between the predicted (solid line) and measured[11] (solid symbols) values of the net lift force due to the jet (Figure 9). The net lift force (Fy) was determined from the actual time histories of the highly unsteady lift force (an example shown in Figure 10 for various angles of attack) resulting from the jet interaction at zero degree angle of attack and computed with the new hybrid RANS/LES turbulence approach.

4.2. Spinning Projectile Case.

In this case, the projectile (40mm grenade) spins clockwise at a rate of 67 Hz looking from the front (see Figure 11). The jet actuation corresponds to one-fourth of the spin cycle from -45° to +45° with zero degree being the positive y-axis. The jet is off during the remaining three-fourths of the spin cycle. The unsteady CFD modeling required about 600 time steps to resolve a full spin cycle. For the part of the spin cycle when the jet is on, the 1000 Hz jet operated for approximately for four cycles. The actual computing time for one full spin cycle of the projectile was about 50 hours using 16 processors (i.e., 800 processor-hours) on an IBM SP3 system for a mesh size about four million grid points. Multiple spin cycles

and, hence, a large number of synthetic jet operations were required to reach the desired periodic time-accurate unsteady result. As will be seen later, some cases were run for as many as 60 spin cycles requiring over 48,000 processor hours of computer time. Computed particle traces (colored by velocity) emanating from the jet into the wake are shown in Figure 12 at a given instant in time for M = 0.24 and α = 0°. The particle traces emanating from the jet interact with the wake flow making it highly unsteady. It shows the flow in the base region to be asymmetric due to the interaction of the unsteady jet.

The computed surface pressures from the unsteady flow fields were integrated to obtain the aerodynamic forces and moments[13] from both unsteady RANS (URANS) as well as the hybrid RANS/LES approach referred here as the LNS. The jet-off unsteady RANS calculations were first obtained and the jets were activated beginning at time, t = 28 ms. Computed normal or lift force (F_Y) and side force (F_Z) were obtained for two different jet velocities, Vj = 31 and 69 m/s and are shown here in Figure 13 for the bigger jet as a function of time. These computed results clearly indicate the unsteady nature of the flow field. When the jet is turned off, the levels of these forces drop to the same levels prior to the jet activation corresponding to the jet-off wake flow. Figure 14 shows the comparison of the predicted lift force using URANS and LNS models. The URANS result clearly shows when the jet is on and when it is off during the spin cycle.

As described earlier, the comparisons for the non-spinning cases showed that the level of lift force predicted by LNS closely matched the data. Here, the addition of spin as well as the jet actuation for part of the spin cycle, further complicates the analysis of the CFD results with LNS. The level of oscillations seen is quite large and the effect of the jet cannot be easily seen in the instantaneous time histories of the unsteady forces and moments. To get the net effect of the jet, unsteady computations were run for many spin cycles of the projectile with the synthetic jets. The CFD results are plotted over only one spin cycle, each subsequent spin cycle was superimposed and a time-averaged result was then obtained over one spin cycle. In all these cases, the jet is on for one-fourth of the spin cycle (time, t=0 to 3.73 ms) and is off for the remainder (three-fourths) of the spin cycle. Figures 15 through 16 show the time-averaged results over a spin cycle. Figure 15 shows the computed lift force again averaged over many spin cycles for the peak jet velocity of 69 m/s. The jet effect can clearly be seen when the jet is on (t=0 to 3.73 ms) even after 5 or 10 spin cycles. The net lift is about 0.17 Newton due to the jet actuation and seems to have converged after 20 spin cycles. For the remainder of the spin cycle, the jet is off; however, the effect of the jet on the wake still persists and this figure shows that lift force (mean value .07 Newton) is still

available. Figure 16 shows the computed averaged lift force after 50 and 60 spin cycles for jet velocities 31 and 69 m/s, respectively. It clearly shows that the larger jet producing larger lift force than the smaller jet when the jet is activated. The lift force can be integrated over time to obtain the impulse. Figure 17 shows the impulse obtained from the lift force as a function of the spin cycles for both jets. As seen here, in both cases it takes about 30 to 40 spin cycles before the impulse asymptotes to a fixed value.

The computed lift force along with other aerodynamic forces and moments, directly resulting from the pulsating jet, were then used in a trajectory analysis[14] and the synthetic micro-jet produced a substantial change in the cross range and thus, provided the desired course correction for the projectile to hit its target.

5. Concluding Remarks

This paper describes a computational study undertaken to determine the aerodynamic effect of tiny synthetic jets as a means to provide the control authority needed to maneuver a projectile at low subsonic speeds. Computed results have been obtained for a subsonic projectile for both non-spinning and spinning cases using time-accurate Navier-Stokes computational techniques and advanced turbulence models. The unsteady jet in the case of the subsonic projectile is shown to substantially alter the flow field both near the jet and the base region that in turn affects the forces and moments even at zero degree angle of attack. The predicted changes in lift force due to the jet match well with the experimental data for various angles of attack from 0° to 4° in the hybrid RANS/LES computations. For the spinning projectile cases, the net *time-averaged* results obtained over the time period corresponding to one spin cycle clearly showed the effect of the synthetic jets on the lift as well as the side forces. The jet interaction effect is clearly seen when the jet is on during the spin cycle. However, these results show that there is an effect on the lift force (although reduced) for the remainder of the spin cycle *even* when the jet is off. This is a result of the wake effects that persist from one spin cycle to another. The impulse obtained from the predicted forces for both jets seem to asymptote after 30 spin cycles.

The results have shown the potential of CFD to provide insight into the jet interaction flow fields and provided guidance as to the locations and sizes of the jets to generate the control authority required to maneuver a spinning munition to its target with precision. This research represents a major increase in capability for determining the unsteady aerodynamics of munitions in a *new area of flow control* and has shown that micro-adaptive flow control with tiny synthetic jets can provide an *affordable* route to *lethal* precision-guided infantry weapons.

References

1. Sahu, J., K.R. Heavey, and E.N. Ferry, "Computational Fluid Dynamics for Multiple Projectile Configurations." *Proceedings of the 3rd Overset Composite Grid and Solution Technology Symposium*, Los Alamos, NM, October 1996.

2. Sahu, J., K.R. Heavey, and C.J. Nietubicz, "Time-Dependent Navier-Stokes Computations for Submunitions in Relative Motion." *6th International Symposium on Computational Fluid Dynamics*, Lake Tahoe, NV, September 1995.

3. Smith, B.L and A. Glezer, "The Formation and Evolution of Synthetic Jets." *Journal of Physics of Fluids*, vol. 10, No. 9, September 1998.

4. Amitay, M., V. Kibens, D. Parekh, and A. Glezer, "The Dynamics of Flow Reattachment over a Thick Airfoil Controlled by Synthetic Jet Actuators." *AIAA Paper No. 99-1001*, January 1999.

5. Arunajatesan, S. and N. Sinha, "Towards Hybrid LES-RANS Computations of Cavity Flowfields." *AIAA Paper No. 2000-0401*, January 2000.

6. Batten, P., U. Goldberg, and S. Chakravarthy, "Sub-grid Turbulence Modeling for Unsteady Flow with Acoustic Resonance." *AIAA Paper 00-0473*, 38th AIAA Aerospace Sciences Meeting, Reno, NV, January 2000.

7. Pulliam, T.H. and J.L. Steger, "On Implicit Finite-Difference Simulations of Three- Dimensional Flow." *AIAA Journal*, vol. 18, no. 2, February 1982, pp. 159–167.

8. Peroomian, O., S. Chakravarthy, S. Palaniswamy, and U. Goldberg, "Convergence Acceleration for Unified-Grid Formulation Using Preconditioned Implicit Relaxation." *AIAA Paper 98-0116*, 1998.

9. Goldberg, U., O. Peroomian, and S. Chakravarthy, "A Wall-Distance-Free K-E Model with Enhanced Near-Wall Treatment." *ASME Journal of Fluids Engineering*, Vol. 120, 1998, pp. 457–462.

10. Batten, P., U. Goldberg, and S. Chakravarthy, "Sub-grid Turbulence Modeling for Unsteady Flow with Acoustic Resonance." *AIAA Paper 00-0473*, 38th AIAA Aerospace Sciences Meeting, Reno, NV, January 2000.

11. Rinehart, C., J.M. McMichael, and A. Glezer, "Synthetic Jet-Based Lift Generation and Circulation Control on Axisymmetric Bodies." *AIAA Paper No. 2002-3168*.

12. McMichael, J., GTRI, Private Communications.

13 Sahu, J., "Unsteady Numerical Simulations of Subsonic Flow over a Projectile with Jet Interaction." *AIAA Paper 2003-1352*, Reno, NV, 6–9 January 2003

14. Costello, M., Oregon State University, private communications.

**Pulsating
Synthetic Jet
Diaphragm**
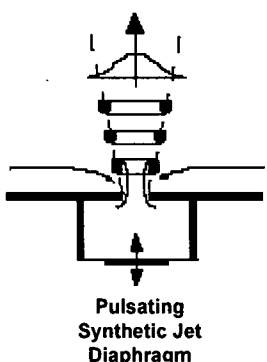
Figure 1. Schematic of a synthetic jet

Lift

*Synthetic
Jet*
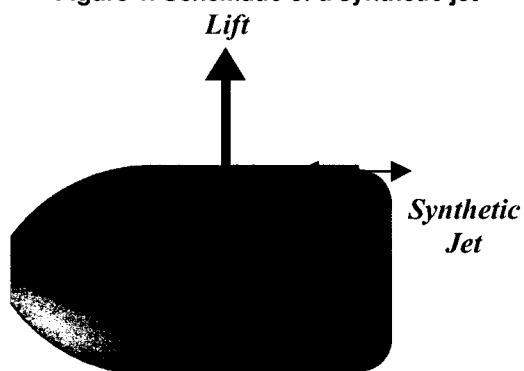
Figure 2. Projectile geometry

Jet

Jet
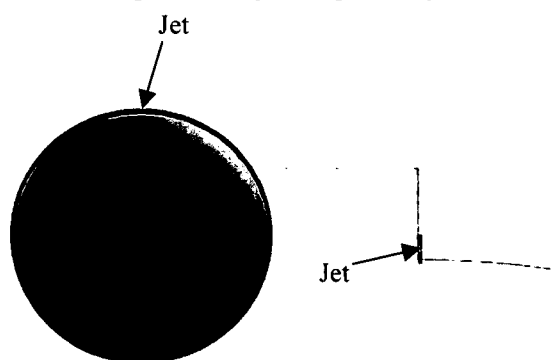
Figure 3. Aft-end geometry showing the jet location
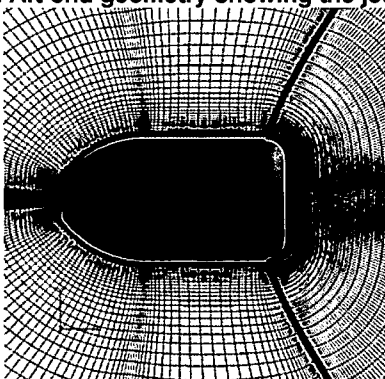

Figure 4. Computational grid near the projectile

TIME=0.0300   Shear Layer

UVW

0   10   20   30   40
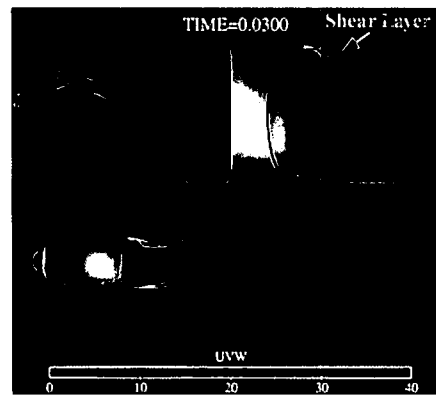
Figure 5. Velocity magnitudes, M=0.11, α = 0°

TIME=0.0300

UVW

0   10   20   30   40
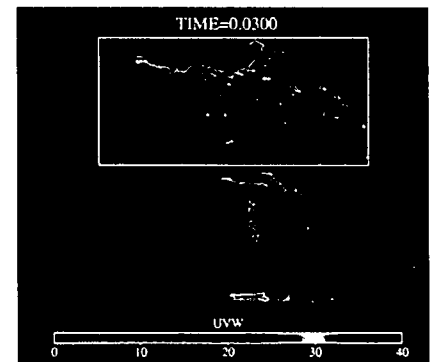
Figure 6. Velocity vectors, M = 0.11, α = 0°

Time   TIME=0.03775   Turb I
0.000 0.010 0.020   0   30   60
   0.005 0.015   15   45

P
100800   101100   101400
   100950   101250
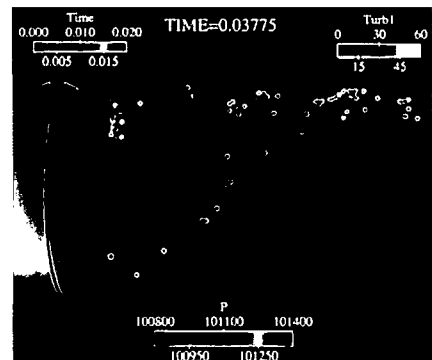
Figure 7. Particle Traces, M = 0.11, α = 0°

TIME=0.0300

P
100800   100950   101100   101250   101400
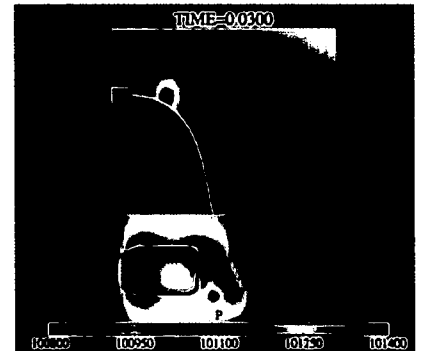
Figure 8. Computed Pressures, M = 0.11, α = 0°
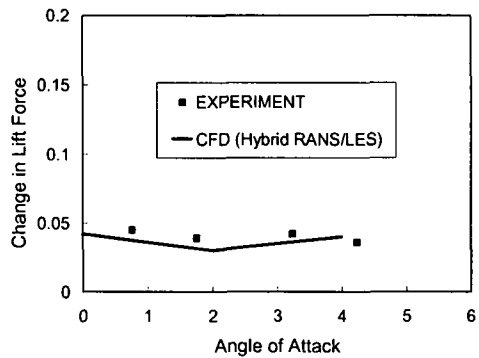
Figure 9. Computed change in lift force due to jet at various angles of attack, M = 0.11
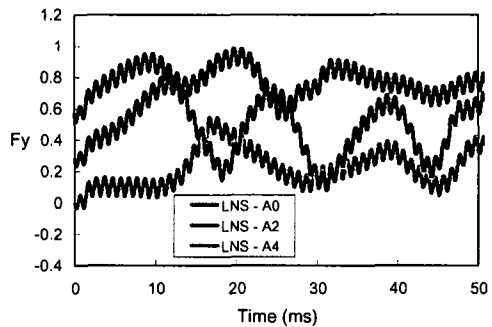
Figure 10. Computed lift force for various angles of attack, M = 0.11
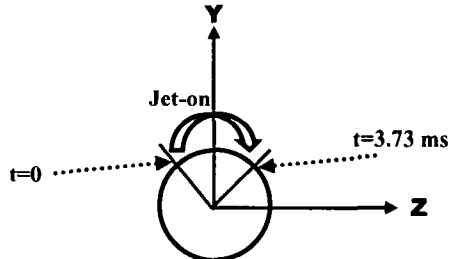
Figure 11. Schematic showing the jet actuation in one spin cycle (view from the front or the nose)
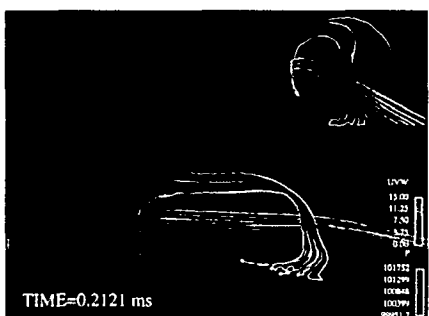
Figure 12. Computed particle traces colored by velocity, jet-on, M = 0.24, α = 0°
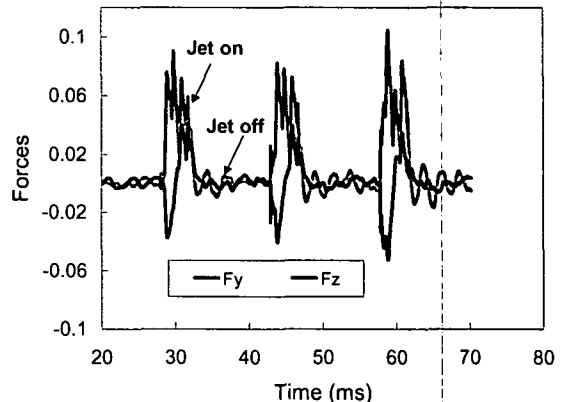
Figure 13. Computed lift and side forces, URANS, M = 0.24, Vj = 69 m/s, α = 0°
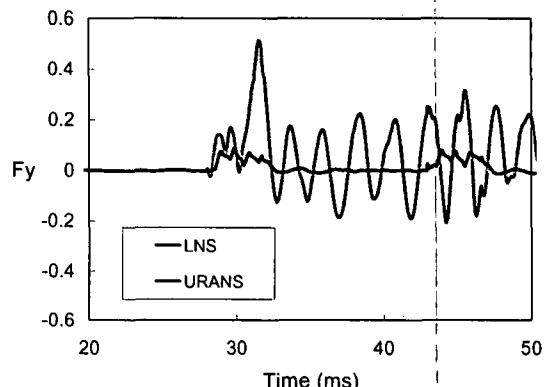
Figure 14. Computed lift forces, URANS and LNS, M = 0.24, Vj = 69 m/s, α = 0°
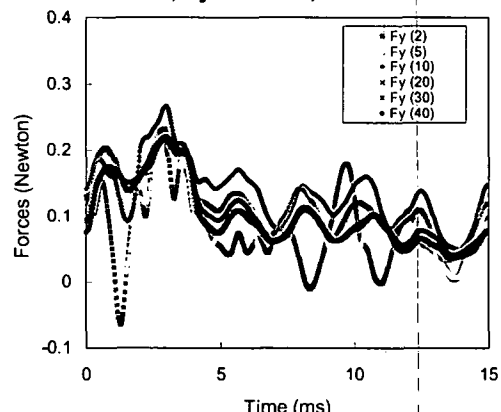
Figure 15. Computed lift force over many spin cycles LNS, Vj = 69 m/s, M = 0.24, α = 0°, Spin = 67 Hz

149
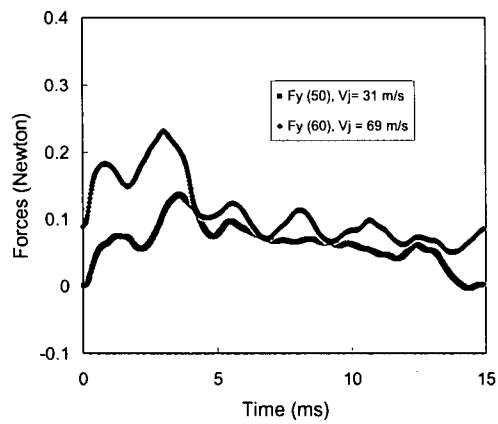
**Figure 16. Computed lift force over many spin, cycles for different jet velocities, LNS, M = 0.24, α = 0°, Spin = 67 Hz.**
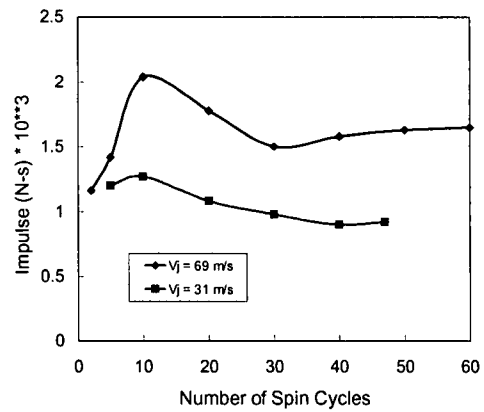
Figure 17. Impulse from the lift force vs. spin cycles for two jet velocities, M = 0.24, α = 0°, Spin = 67 Hz

150